Plant Mitochondrial-Targeted Gene Delivery by Peptide/DNA Micelles Quantitatively Surface-Modified with Mitochondrial Targeting and Membrane-Penetrating Peptides

AUTHOR(S):

Abe, Naoya; Fujita, Seiya; Miyamoto, Takaaki; Tsuchiya, Kousuke; Numata, Keiji

CITATION:

Abe, Naoya ...[et al]. Plant Mitochondrial-Targeted Gene Delivery by Peptide/DNA Micelles Quantitatively Surface-Modified with Mitochondrial Targeting and Membrane-Penetrating Peptides. Biomacromolecules 2023, 24(8): 3657-3665

ISSUE DATE:

2023-06-29

URL:

http://hdl.handle.net/2433/286261

Biomacromolecules

pubs.acs.org/Biomac

Article

Plant Mitochondrial-Targeted Gene Delivery by Peptide/DNA Micelles Quantitatively Surface-Modified with Mitochondrial Targeting and Membrane-Penetrating Peptides

Naoya Abe, Seiya Fujita, Takaaki Miyamoto, Kousuke Tsuchiya, and Keiji Numata*

Cite This: *Biomacromolecules* 2023, 24, 3657−3665

Read Online

ACCESS | Metrics & More | Article Recommendations | Supporting Information

ABSTRACT: Plant mitochondria play essential roles in metabolism and respiration. Recently, there has been growing interest in mitochondrial transformation for developing crops with commercially valuable traits, such as resistance to environmental stress and shorter fallow periods. Mitochondrial targeting and cell membrane penetration functions are crucial for improving the gene delivery efficiency of mitochondrial transformation. Here, we developed a peptide-based carrier, referred to as Cytcox/KAibA-Mic, that contains multifunctional peptides for efficient transfection into plant mitochondria. We quantified the mitochondrial targeting and cell membrane-penetrating peptide modification rates to control their functions. The modification rates were easily determined from high-performance liquid chromatography chromatograms. Additionally, the gene carrier size remained constant even when the mitochondrial targeting peptide modification rate was altered. Using this gene carrier, we can quantitatively investigate the relationships between various peptide modifications and transfection efficiency and optimize the gene carrier conditions for mitochondrial transfection.

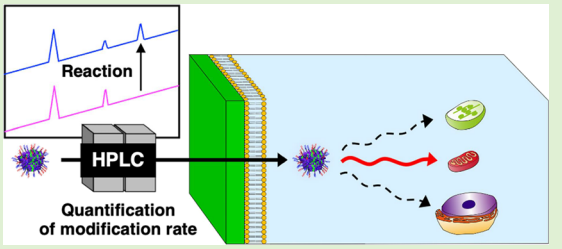

INTRODUCTION

With increasing food demand caused by population explosion, food supply cannot meet food demand due to climate change and a decrease in farmland. The development of crops with effective traits for improving productivity, such as environmental resistance and a shorter fallow period, is required.[1−3] To dramatically change the traits of plants, gene engineering has been markedly developed.[4−6] Although gene engineering research has mainly been focused on the nucleus, mitochondrial and plastid genome editing has recently attracted attention. While most genes exist in the nucleus, mitochondria and plastids have unique genes different from those in the nucleus. In particular, mitochondria synthesize adenosine triphosphate and play a significant role in energy production in organisms. Editing the mitochondrial genome in plants is expected to produce plants with commercially beneficial traits, such as cytoplasmic male sterility and environmental stress resistance.[7−9] However, a mitochondrial transformation method has not yet been established because there is no way to select cells with transformed mitochondria. Therefore, mitochondrial transformation requires a higher efficiency than the transformation of the nucleus and the other organelles. Since existing methods, such as particle bombardment, cannot target mitochondria due to their small size and dynamic movement, genes must be precisely delivered to mitochondria.

Natural peptides are composed of 20 natural amino acids and form characteristic secondary structures to maintain cellular activities.[10] In living cells, peptides play various roles depending on their amino acid sequences and structures. Signal peptides deliver synthesized proteins to each defined site.[11−13] For example, mitochondrial proteins with presequences (signal peptides) at the N-terminus are synthesized by ribosomes in the cytosol, and these proteins are delivered to mitochondria. The translocation occurs because a translocase on the outer mitochondrial membrane recognizes the amino acid sequence and the secondary structure of the signal peptides. Cytcox (MLSLRQSIRFFK), derived from cytochrome *c* oxidase subunit IV, is a mitochondrial targeting peptide.[14] Cytcox is relatively short for a mitochondrial targeting peptide and has been used for gene transfection into mitochondria.[15−18] Furthermore, since peptides are also easily hydrolyzed by proteases in cells, peptides do not stay in cells for a long time and can be designed for toxicity control. In contrast, synthetic polymers cannot form specific secondary structures as can peptides, and their degradability is much lower than that of biopolymers. Taking advantage of these merits of peptides, many applications of peptides as nanocarriers to replace synthetic polymers have been reported in recent years.[19,20] Cationic peptides containing arginine and

Received: April 18, 2023
Revised: May 18, 2023
Published: June 29, 2023

https://doi.org/10.1021/acs.biomac.3c00391
Biomacromolecules 2023, 24, 3657−3665

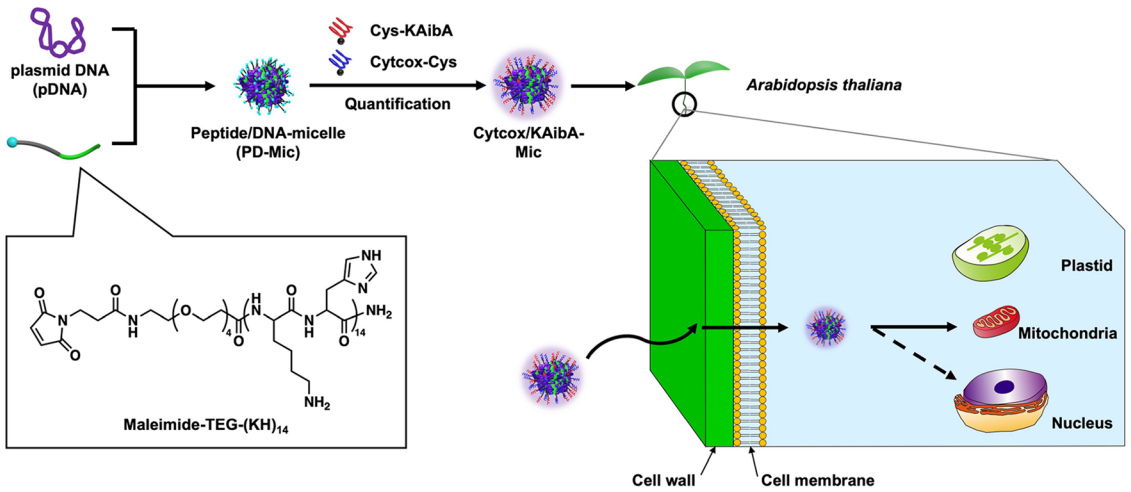

Figure 1. Schematic illustration of the preparation and mitochondrial transfection of Cytcox/KAibA-Mic in plants.

lysine can form complexes with anionic DNA by electrostatic interactions.[21−23] Additionally, genes can be introduced into animal and plant cells using peptide/DNA complexes with functional peptides, such as organelle targeting peptides and membrane-penetrating peptides.[15,17,24−30] We have previously developed a gene carrier, peptide-DNA micelle (PD-Mic), that can be modified with two types of functional peptides.[29] PD-Mic can be easily prepared by simply mixing plasmid DNA (pDNA) and peptide solution, MAL-TEG-$(KH)_{14}$ (MAL: maleimide, TEG: tetraethylene glycol). Functional peptides containing Cys can react with the MAL group on the surface of PD-Mic. For gene transfection into plant mitochondria, it has been clarified that the functions of mitochondrial targeting and membrane penetration are critical.[15] However, high membrane permeability decreases cell selectivity and restricts transfection efficiency.[18] The functions of mitochondrial targeting and membrane penetration need to be optimized to improve transfection efficiency.

In this report, we developed a gene carrier that quantitatively controlled the modification rates of mitochondrial targeting and membrane-penetrating peptides (Figure 1). These modification rates could be quantified using high-performance liquid chromatography (HPLC) in vitro. The quantification of the protein expression level at various mitochondrial targeting peptide modification rates confirmed that the modification rates could be correctly controlled as calculated by HPLC. Furthermore, this gene carrier was so stable that it maintained its size at various peptide modification rates. By utilizing this gene carrier, we could quantitatively analyze the relationships between the functions of modifying peptides and their mitochondrial transfection efficiency.

EXPERIMENTAL SECTION

Peptide Synthesis. MAL-TEG-$(KH)_{14}$ (Maleimide-TEG-KHKHKHKHKHKHKHKHKHKHKHKHKH-NH_2, M_w = 4130) was synthesized via standard solid-phase peptide synthesis[31] using 9-fluorenyl methoxycarbonyl (Fmoc) amino acids (Figure S1A). The Fmoc amino acids used in this report were purchased from Watanabe Chemical Industries (Hiroshima, Japan) and Tokyo Chemical Industry (Tokyo, Japan). This synthesis was performed with an automatic synthesizer (INITIATOR+ Alstra, Biotage AB, Uppsala, Sweden). After synthesis, MAL-TEG-$(KH)_{14}$ was purified using reverse-phase high-performance liquid chromatography (RP-HPLC). The purity of this peptide was determined to be greater than 95% by RP-HPLC analysis (Figure S1B). The mobile phase comprised 10−20% acetonitrile (CH_3CN) (FUJIFILM Wako Pure Chemical, Osaka, Japan) containing 0.1% trifluoroacetic acid (TFA) (FUJIFILM Wako Pure Chemical). The flow rate was 1.0 mL/min. The detection wavelength was 220 nm. This RP-HPLC analysis was performed with an HPLC system consisting of an SIL-20 AC autosampler, an LC-20 AD gradient pump, a CTO-20AC column oven, and an SPD-M20A UV/vis detector (Shimadzu Corporation, Kyoto, Japan). The molecular weight was confirmed through matrix-assisted laser desorption/ionization-time-of-flight mass spectrometry (MALDI-TOF MS). Mitochondrial targeting peptides Cytcox-Cys (MLSLRQSIRFFKC-NH_2) and Cytcox-$(KH)_9$ (MLSLRQSIRFFKKHKHKHKHKHKHKHKHKH-NH_2) and the cell membrane-penetrating peptide Cys-KAibA (Ac-CKXAKXAK-XA-NH_2, X = 2-aminoisobutyric acid (Aib)) were synthesized using Fmoc solid-phase peptide synthesis by the Research Resources Division of RIKEN Center for Brain Science (Wako, Japan).

Plant Materials and Growth Conditions. The seeds of wild-type *Arabidopsis thaliana* (*A. thaliana*) were sterilized in ethanol/water (70% v/v) for 1 min and then twice in bleach/water (5% v/v) for 4 min and then rinsed six times with sterilized water. After that, the seeds were stored at 4 °C for at least 2 days. The seeds were grown on half-strength Murashige and Skoog (1/2 MS) medium containing MS salts (Sigma-Aldrich, St. Louis, MO) (2.2 g/L), 2-morpholinoethanesulfonic acid (MES) (Dojindo Molecular Technologies, Inc., Kumamoto, Japan) (0.5 g/L, adjusted to pH 5.7 with potassium hydroxide (KOH) (FUJIFILM Wako Pure Chemical)), sucrose (FUJIFILM Wako Pure Chemical) (10 g/L), and agarose (FUJIFILM Wako Pure Chemical) (0.8% w/v) under daylength conditions of 16 h of light/8 h of darkness at 22 °C. Seedlings were harvested 6 days after germination and used for all experiments.

Plasmid DNA Constructs. In this study, four types of pDNA, *pDONR-Cox2-RLuc*, *pATMTTF1*, *pDONR-35S-RLuc*, and *pDONR-35S-GFP*, were used (Figure S2A−D). The cytochrome *c* oxidase subunit II (Cox2) promoter was used to identify mitochondrial expression, and *pDONR-Cox2-RLuc* contained the Cox2 promoter. Additionally, *pATMTTF1* contained the *A. thaliana* Cox1 promoter, which also functions in mitochondria. The Cauliflower mosaic virus 35S promoter was used for identifying nuclear expression, and *pDONR-35S-RLuc* and *pDONR-35S-GFP* contained the 35S promoter. To evaluate transfection into mitochondria or nuclei, we used *pDONR-Cox2-RLuc* and *pDONR-35S-RLuc*, which encode the *Renilla* luciferase (*RLuc*) gene, and *pATMTTF1* and *pDONR-35S-GFP*, which encode the green fluorescent protein (*GFP*) gene.

Preparation and Characterization of PD-Mic. A 2 mg/mL MAL-TEG-$(KH)_{14}$ aqueous solution was added to Milli-Q water containing pDNA (40 μg) to produce solutions with N/P ratios (defined as the molar ratio of cationic peptide nitrogen to anionic DNA phosphate) from 0.5 to 4. The final volume and pDNA

https://doi.org/10.1021/acs.biomac.3c00391
Biomacromolecules 2023, 24, 3657−3665

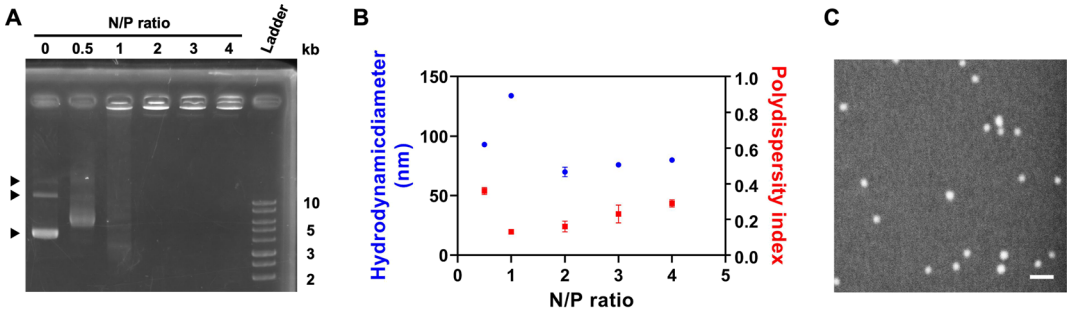

Figure 2. Characterization of the PD-Mic at various N/P ratios. (A) EMSA results of naked pDNA (N/P = 0) and PD-Mic (N/P = 0.5−4). The arrows indicate different conformations (top, open-circular; middle, linear; bottom, supercoiled) of *pDONR-Cox2-RLuc* (8.6 kb) used in the analysis. (B) Hydrodynamic diameter (blue) and polydispersity index (red) of PD-Mic at N/P 0.5−4 (n = 3). The vertical bars indicate the standard deviations. (C) FE-SEM image of PD-Mic (N/P 2). The scale bar represents 200 nm.

concentration were fixed at 800 μL and 50 μg/mL, respectively. The PD-Mic solutions (800 μL) prepared with each N/P ratio were vortexed for 10 s and incubated for 30 min at 25 °C to stabilize them, and then they were characterized by the electrophoretic mobility shift assay (EMSA), dynamic light scattering (DLS), zeta potential measurements, and field-emission scanning electron microscopy (FE-SEM).

For the EMSA, sample solutions (5 μL) were mixed with 6× loading buffer double dye (1 μL) (FUJIFILM Wako Pure Chemical) containing Tris−HCl (10 mM, pH 7.5), ethylenediaminetetraacetic acid (EDTA, 50 mM), xylene cyanol FF (0.3% w/v), Orange G (0.3% w/v), and Ficoll PM400 (15% w/v). The mixtures were subjected to agarose gel (1% w/v) (NIPPON GENE Co., Ltd., Toyama, Japan) electrophoresis at 100 V for 25 min in tris-acetate-EDTA (TAE) buffer (KANTO CHEMICAL Co., Inc., Tokyo, Japan), followed by staining with ethidium bromide for 30 min. The PD-Mic hydrodynamic diameter was characterized by DLS measurements using a Zetasizer Nano ZS instrument (Malvern Instruments Ltd., Worcestershire, UK). The measurements were performed in a plastic cell (DTS1070) using a 633 nm He-Ne laser at 25 °C with a backscatter detection angle of 173° to estimate the hydrodynamic diameter in terms of the Z-average size and polydispersity index (PDI). Zeta potential measurements were performed three times at 25 °C to obtain the average zeta potential values using the same instruments as those used for the DLS measurements. The morphology of the prepared micelles was observed with an FE-SEM, GeminiSEM 300 (Carl Zeiss, Oberkochen, Germany). A micelle solution (0.5 μL) was dripped on a silicon wafer, and then the liquid was lyophilized. The sample was subjected to FE-SEM observation with an acceleration voltage of 1 kV.

Preparation and Characterization of Peptide-Modified Micelles. The PD-Mic, prepared at N/P 2, was modified with Cytcox-Cys or Cys-KAibA in Bis-Tris buffer (Dojindo Molecular Technologies, Inc.) (1 mM, pH 7.0) to obtain Cytcox-modified micelles or KAibA-modified micelles, respectively. Then, 10 μL of 500 μM Cytcox-Cys or Cys-KAibA was added to the PD-Mic solution. The final concentration of MAL-TEG-$(KH)_{14}$ was fixed at 18.90 μM, whereas the concentrations of the Cytcox peptide and the KAibA peptide were adjusted to 6.10 μM. The mixture (final volume, 820 μL) was left to rest at 25 °C for 1 h. The Cytcox/KAibA-modified micelles were simultaneously modified with Cytcox and KAibA in Bis-Tris buffer (1 mM, pH 7.0). Five microliters of Cytcox-Cys and Cys-KAibA was added to the PD-Mic solution. The final concentration of MAL-TEG-$(KH)_{14}$ was 18.90 μM, whereas the concentrations of the Cytcox peptide and the KAibA peptide were adjusted to 3.05 μM. The mixture (820 μL) was left to rest at 25 °C for 1 h. The reaction mixture containing each peptide-modified micelle was directly used for characterization and transfection experiments. The peptide modification rates of the peptide-modified micelles were analyzed with RP-HPLC. The modification rates were defined as the ratio of the number of reacted MAL groups to the number of all MAL groups in solution and calculated by comparing the peak area of each peptide in the HPLC chromatograms before and after modification. The mobile phase comprised 5.0−52.5% CH_3CN containing 0.1% TFA. The flow rate was 1.0 mL/min. These RP-HPLC analyses were performed using the same equipment as that used for peptide purification. Characterization of the peptide-modified micelles by MALDI-TOF MS, DLS, and FE-SEM was performed in the same way as described above.

Infiltration of Peptide-Modified Micelles in Plants. A peptide-modified micelle solution was added to 10 seedlings of *Arabidopsis thaliana* (*A. thaliana*), and then the seedlings were placed in a reduced pressure environment (−0.08 MPa) for one minute, then in a pressurized environment (0.08 MPa) for one minute. After that, the seedlings were left to soak in the micelle solution for one hour and then returned to 1/2 MS medium.

Observation of GFP Expression. Peptide-modified micelles (Cytcox-Mic, KAibA-Mic, and Cytcox/KAibA-Mic) were prepared from GFP-coding pDNA (*pATMTTF1*, *pDONR-35S-GFP*) by the method described above. Twenty-four hours after infiltration, the mitochondria of the seedlings were stained with 100 nM MitoTracker Red CMXRos (Thermo Fisher, U.S.A.) for 45 min at 25 °C, and then the main root cells of the seedlings were observed with a confocal laser scanning microscope (CLSM), LSM880 (Carl Zeiss, Oberkochen, Germany).

Transfection Efficiency Assay. For transfection experiments based on luciferase expression, peptide-modified micelles were prepared from *Renilla* luciferase-coding pDNA (*pDONR-Cox2-RLuc*, *pDONR-35S-RLuc*). Twenty-four hours after infiltration, each group of seedlings was homogenized in *Renilla* Luciferase Assay Lysis Buffer (100 μL, Promega, Madison, WI, U.S.A.). The lysate was centrifuged at 15,000 rpm for 5 min, and the supernatant (100 μL) was added to a mixture (100 μL) of *Renilla* Luciferase Assay Substrate (Promega) and *Renilla* Luciferase Assay Buffer (Promega). Immediately after vortexing, the *Renilla* luciferase expression level in the mixture was evaluated by measuring the luminescence intensity in relative light units (RLUs) using a luminometer (GloMax 20/20, Promega). The supernatant obtained from the lysate was diluted with Milli-Q water and mixed with Bradford reagent to quantify the protein amount based on the absorbance at 595 nm. Each RLU was divided by the protein amount to obtain an RLU/mg value. The corrected RLU/mg values obtained from six biologically independent samples were used for the quantitative evaluation of transfection efficiency.

Statistical Analysis. The statistical significance of differences in transfection efficiency of peptide-modified micelles was evaluated by Dunnett's multiple comparisons tests. The level of significance was set at $P > 0.05$ (n.s.), $P < 0.05$ (*), $P < 0.01$ (**), and $P < 0.001$ (***).

RESULTS AND DISCUSSION

Characterization of PD-Mic Formation. The PD-Mic solutions were prepared by mixing MAL-TEG-$(KH)_{14}$ solution and pDNA (*pDONR-Cox2-RLuc*) solution with N/P ratios from 0.5 to 4. The properties of the PD-Mic at each N/P ratio

https://doi.org/10.1021/acs.biomac.3c00391
Biomacromolecules 2023, 24, 3657−3665

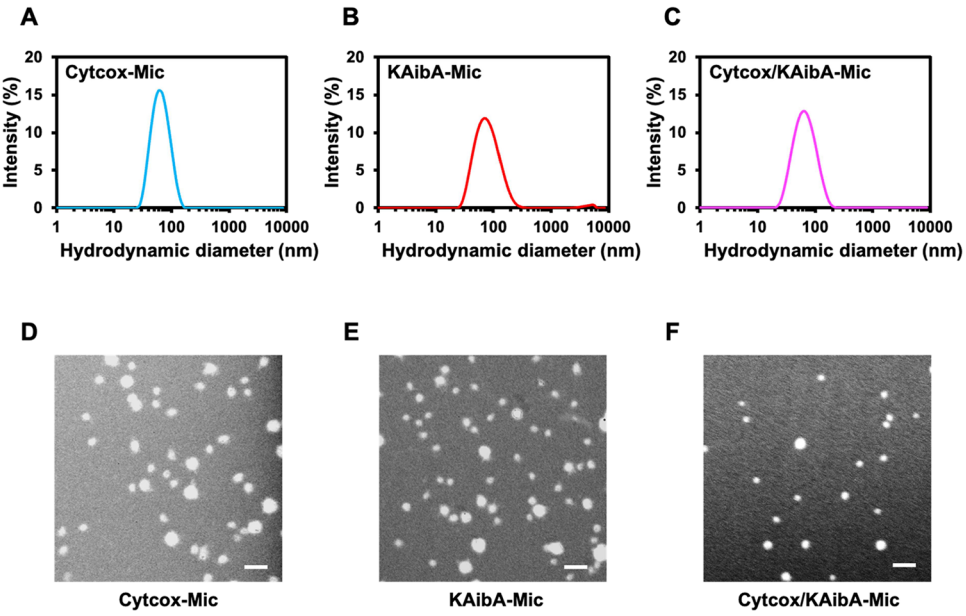

Figure 3. Characterization of peptide-modified micelles. (A–C) Hydrodynamic diameter of Cytcox-Mic, KAibA-Mic, and Cytcox/KAibA-Mic based on DLS measurement (n = 3). (D–F) FE-SEM images of (D) Cytcox-Mic, (E) KAibA-Mic, and (F) Cytcox/KAibA-Mic. Scale bars represent 200 nm.

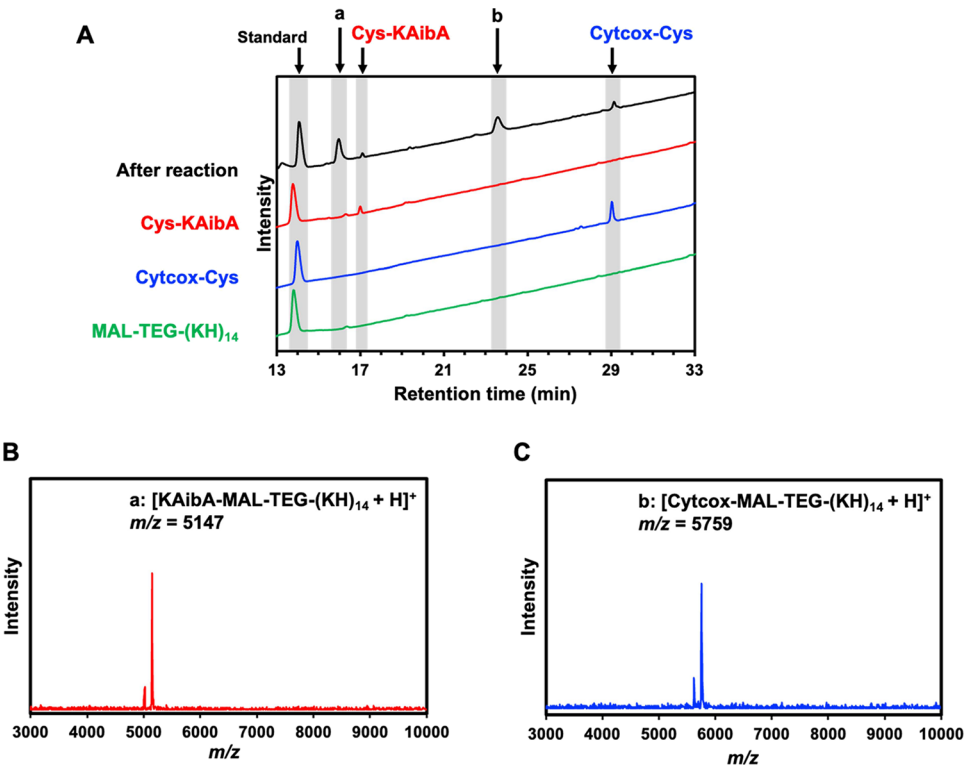

Figure 4. Quantification of Cytcox and KAibA modification rates. (A) RP-HPLC chromatograms of the peptide solution before or after modification. Each solution was eluted by a mixed mobile phase with a linear gradient of CH_3CN/water containing 0.1% TFA (5/95 to 47.5/52.5 over 47.5 min) (n = 3). Boc-Gly-OH was used as the internal standard. (B, C) Identification of products after the reaction of MAL-TEG-$(KH)_{14}$ with (B) Cys-KAibA and (C) Cytcox-Cys. These MALDI-TOF MS spectra show the molecular weights of peaks "a" and "b" in Figure 4A.

were analyzed with EMSA, DLS, and FE-SEM. In the EMSA, the bands of free DNA (N/P 0 lane) faded as the N/P ratio increased, and then the band completely shifted at N/P 2 (Figure 2A). This movement indicated that all pDNA interacted with MAL-TEG-$(KH)_{14}$ at N/P ratios of more than 2. To optimize the N/P ratio, the hydrodynamic diameters of the PD-Mic at different N/P ratios were analyzed with DLS. The minimum diameter value was 70 ± 2 nm (PDI: 0.16 ± 0.03) at N/P 2 (Figure 2B). At N/P 1, the PD-Mic was probably more unstable compared with the other N/P ratio because the charges of MAL-TEG-$(KH)_{14}$ and pDNA were equal. Therefore, the PD-Mic at N/P 1 was larger than that at

https://doi.org/10.1021/acs.biomac.3c00391
Biomacromolecules 2023, 24, 3657−3665

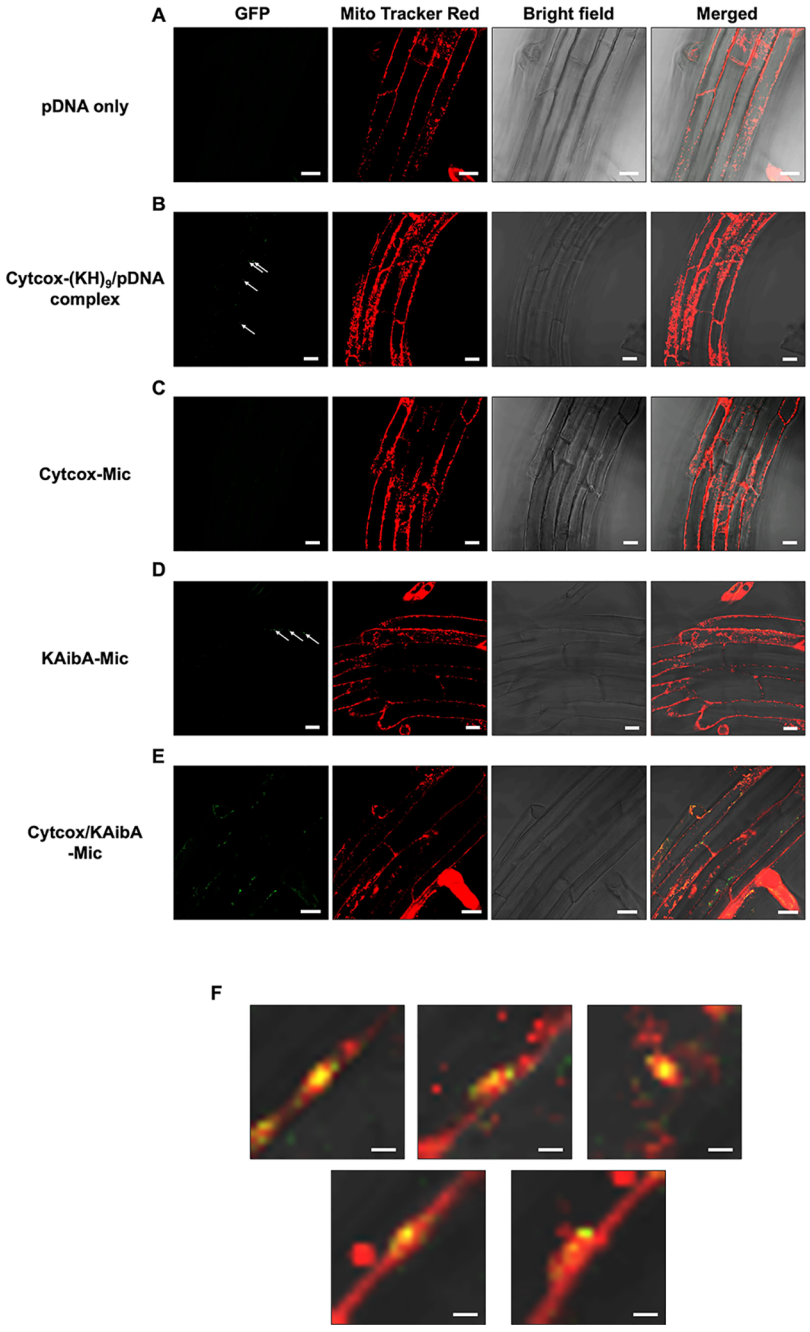

Figure 5. Representative CLSM images of *A. thaliana* root cells 24 h after infiltration with pDNA (A) and peptide-modified micelles [Cytcox-$(KH)_9$/pDNA complex (mito-GFP): (B), Cytcox-Mic (mito-GFP): (C), KAibA-Mic (mito-GFP):(D), and Cytcox/KAibA-Mic (mito-GFP): (E)]. The white arrows in (B) and (D) indicate some of expressed GFP. (F) Enlarged images of several mitochondria with GFP expression in (E). Mitochondria were stained with MitoTracker Red CMXRos. Scale bars represent 20 μm in (A−E) and 2 μm in (F).

N/P 0.5, 2, 3, and 4. There were no significant differences between the PD-Mic sizes at N/P 2−4. The PD-Mic at N/P 2 was spherical, and the diameter was 50−65 nm according to the FE-SEM observation (Figure 2C). Smaller particles are more likely to penetrate the cell wall, so N/P 2 was selected for the subsequent experiments.

Characterization of Peptide-Modified Micelles. Cytcox-Cys and Cys-KAibA were added to the PD-Mic solution to modify the PD-Mic surface with Cytcox and KAibA. This modification occurred through the reaction between thiol and maleimide. According to the DLS measurements, the hydrodynamic diameter of Cytcox and KAibA-modified PD-Mic (Cytcox/KAibA-Mic) was 63 ± 2 nm (PDI: 0.20 ± 0.01) (Figure 3C and Table S2). Additionally, the hydrodynamic diameters of Cytcox-modified PD-Mic (Cytcox-Mic) and KAibA-modified PD-Mic (KAibA-Mic) were 60 ± 1 nm (PDI: 0.12 ± 0.01) and 72 ± 1 nm (PDI: 0.19 ± 0.01), respectively (Figure 3A,B and Table S2). In addition, the three types of peptide-modified micelles were found to be spherical by FE-SEM observation (Figure 3D−F). The sizes of the peptide-modified micelles did not change from that of PD-Mic, indicating that it is possible to modify the PD-Mic surface with Cytcox and KAibA without significantly changing the PD-Mic morphology. Furthermore, there was no significant difference

https://doi.org/10.1021/acs.biomac.3c00391
Biomacromolecules 2023, 24, 3657−3665

in the zeta potentials of Cytcox-Mic, KAibA-Mic, and Cytcox/KAibA-Mic (Table S3).

The peptide modification rates were analyzed using HPLC. For Cytcox/KAibA-Mic, the modification rates of Cytcox and KAibA were calculated as 8.9 ± 1.2 and 10.0 ± 4.0%, respectively (Figure 4A). In the case of Cytcox-Mic, 9.5 ± 0.4% of MAL-TEG-$(KH)_{14}$ reacted with Cytcox-Cys, and in the case of KAibA-Mic, 9.8 ± 0.2% of MAL-TEG-$(KH)_{14}$ reacted with Cys-KAibA (Figure S4). From these chromatograms, the products of the thiol-maleimide reaction were detected. By measuring the molecular weight of the eluate for each peak, the peaks at 16.0 and 23.5 min were attributed to KAibA-MAL-TEG-$(KH)_{14}$ and Cytcox-MAL-TEG-$(KH)_{14}$, respectively (Figure 4B,C). These data indicated that the modification of the micelles with the functional peptides proceeded successfully.

Transfection of Peptide-Modified Micelles into Plant Mitochondria. Transfection was evaluated by examining the expression of a reporter gene. We used *pATMTTF1* encoding GFP with a mitochondrial promoter as pDNA in this experiment. Here, the peptide-modified micelles containing *pATMTTF1* were called Cytcox/KAibA-Mic (mito-GFP), Cytcox-Mic (mito-GFP), and KAibA-Mic (mito-GFP), respectively. As indicated by the DLS measurements, the hydrodynamic diameters of Cytcox/KAibA-Mic (mito-GFP), Cytcox-Mic (mito-GFP), KAibA-Mic (mito-GFP), and the peptide/pDNA complex prepared by mixing Cytcox-$(KH)_9$ peptide and pDNA (Cytcox-$(KH)_9$/pDNA complex (mito-GFP)) ranged from 70−85 nm (Table S2). The Cytcox-$(KH)_9$/pDNA complex has been reported to be capable of transfection into plant mitochondria.[17] These peptide-modified micelles and complexes were infiltrated into the seedlings of *A. thaliana*, and the root cells were observed with CLSM. For the root cells that were infiltrated with naked pDNA and Cytcox-Mic (mito-GFP), fluorescence was not observed (Figure 5A,C). On the other hand, in the root cells that were infiltrated with the Cytcox-$(KH)_9$/pDNA complex (mito-GFP) and KAibA-Mic (mito-GFP), slight GFP fluorescence was detected (Figure 5B,D). Compared to these results, the CLSM images shown in Figure 5E indicated that Cytcox/KAibA-Mic (mito-GFP) was superior in terms of transfection into plant mitochondria. GFP was expressed in some cells. These images showed that Cytcox/KAibA-Mic, the DNA carrier modified with Cytcox and KAibA on the surface, could introduce pDNA into mitochondria, resulting in the reporter gene being expressed in mitochondria. Furthermore, Cytcox/KAibA-Mic might deliver pDNA more efficiently than the other peptide-modified micelles and complexes because more GFP-expressing cells were observed in the seedlings infiltrated with Cytcox/KAibA-Mic.

To support GFP expression in mitochondria, we also examined GFP expression in the nucleus. We used *pDONR-35S-GFP* instead of *pATMTTF1* and evaluated GFP expression using the same method as that used for *pATMTTF1*. Here, the peptide-modified micelles containing *pDONR-35S-GFP* are called Cytcox-$(KH)_9$/pDNA complex (nuc-GFP), Cytcox-Mic (nuc-GFP), KAibA-Mic (nuc-GFP), and Cytcox/KAibA-Mic (nuc-GFP), respectively. According to the DLS measurements, the hydrodynamic diameters of the Cytcox-$(KH)_9$/pDNA complex (nuc-GFP), Cytcox-Mic (nuc-GFP), KAibA-Mic (nuc-GFP), and Cytcox/KAibA-Mic (nuc-GFP) were 71 ± 2 nm (PDI: 0.22 ± 0.01), 92 ± 1 nm (PDI: 0.29 ± 0.03), 84 ± 2 nm (PDI: 0.23 ± 0.01), and 88 ± 1 nm (PDI: 0.23 ± 0.01), respectively. For the root cells infiltrated with naked pDNA, the Cytcox-$(KH)_9$/pDNA complex (nuc-GFP), and Cytcox-Mic (nuc-GFP), GFP fluorescence was not observed (Figure S5A−C). On the other hand, in the root cells infiltrated with KAibA-Mic (nuc-GFP) and Cytcox/KAibA-Mic (nuc-GFP), GFP was expressed throughout (Figure S5D, E). When *pDONR-35S-GFP* is transported to the nucleus, the transcribed mRNA translocates to a ribosome, and the protein is expressed in the cytosol. Additionally, it has been reported that a gene carrier modified with KAibA can deliver pDNA to the nucleus. Thus, the CLSM images showed that KAibA-Mic and Cytcox/KAibA-Mic delivered the pDNA to the nucleus. In addition, GFP was expressed in a region distinctly different from that of *pATMTTF1*. This difference indicated that the two promoters, Cox2 and 35S, functioned correctly in the mitochondria and the nucleus, respectively.

Quantitative Transfection Efficiency Test. The *Renilla* luciferase (RLuc) expression level was quantified to evaluate the transfection efficiency of the peptide-modified micelles and complexes. First, we evaluated transfection efficiency to the nucleus to investigate whether the micelles and complexes could penetrate into the plant cell through its plasma membrane and cell wall. Carriers with membrane permeability are known to be able to penetrate the cell and even the nucleus.[29] The micelles and complexes were prepared using *pDONR-35S-RLuc* with a 35S promoter that functions in the nucleus. Here, the peptide-modified micelles containing *pDONR-35S-RLuc* were called Cytcox/KAibA-Mic (nuc-RLuc), Cytcox-Mic (nuc-RLuc), KAibA-Mic (nuc-RLuc), and Cytcox-$(KH)_9$/pDNA complex (nuc-RLuc), respectively. The hydrodynamic diameter of the micelles and complex was 109 ± 3 nm (PDI: 0.12 ± 0.01) for Cytcox/KAibA-Mic (nuc-RLuc), 108 ± 3 nm (PDI: 0.17 ± 0.00) for Cytcox-Mic (nuc-RLuc), 112 ± 3 nm (PDI: 0.11 ± 0.02) for KAibA-Mic (nuc-RLuc), and 99 ± 3 nm (PDI: 0.12 ± 0.01) for the Cytcox-$(KH)_9$/pDNA complex (nuc-RLuc) (Table S2). Seedlings of *A. thaliana* were infiltrated with each micelle solution, and then the transfection efficiency into the nucleus was evaluated under each condition. Seedlings treated with Cytcox/KAibA-Mic (nuc-RLuc) and KAibA-Mic (nuc-RLuc) had significantly higher RLuc expression levels. This result indicated that Cytcox/KAibA-Mic and KAibA-Mic could penetrate the cell, although the KAibA modification rate was as low as 10%. Compared to Cytcox/KAibA-Mic (nuc-RLuc) and KAibA-Mic (nuc-RLuc), KAibA-Mic (nuc-RLuc) showed a higher expression level. It was anticipated that the luciferase expression level was lower in Cytcox/KAibA-Mic (nuc-RLuc) than in KAibA-Mic (nuc-RLuc) because a portion of Cytcox/KAibA-Mic (nuc-RLuc) was transfected into mitochondria via Cytcox.

Transfection efficiency to mitochondria was also evaluated by quantifying the RLuc expression level. The micelles were prepared using *pDONR-Cox2-RLuc*, which expresses RLuc when transported into mitochondria. Here, the micelles were called Cytcox-$(KH)_9$/pDNA complex (mito-RLuc), Cytcox-Mic (mito-RLuc), KAibA-Mic (mito-RLuc), and Cytcox/KAibA-Mic (mito-RLuc), respectively. In this transfection efficiency assay, Cytcox-Mic (mito-RLuc) and KAibA-Mic (mito-RLuc) showed little ability to deliver pDNA into plant mitochondria, whereas Cytcox/KAibA-Mic (mito-RLuc) showed a superior ability (Figure 6). KAibA-Mic showed high efficiency in transfection to the nucleus but not to mitochondria. These results indicated that pDNA could not be

https://doi.org/10.1021/acs.biomac.3c00391
Biomacromolecules 2023, 24, 3657−3665

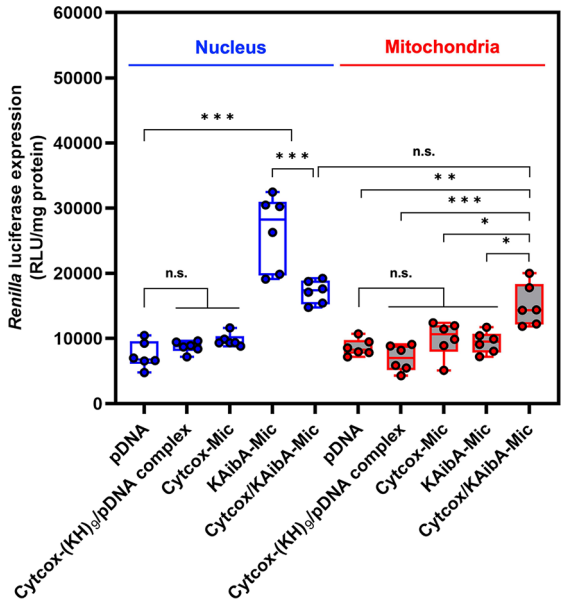

Figure 6. Transfection efficiency to the nucleus or mitochondria of the peptide-modified micelles and naked pDNA based on the *Renilla* luciferase expression levels. This experiment used *pDONR-35S-RLuc* for the nucleus and *pDONR-Cox2-RLuc* for mitochondria. Statistical significance was set at $P > 0.05$ (n.s.), $P < 0.05$ (*), $P < 0.01$ (**), and $P < 0.001$ (***) based on Dunnett's multiple comparison tests ($n = 6$).

transported in mitochondria simply by a nonspecific interaction with the plasma membrane, and Cytcox worked well as a mitochondrial transit signal on the Cytcox/KAibA-Mic surface. Furthermore, Cytcox/KAibA-Mic (mito-RLuc) showed a higher transfection efficiency than the Cytcox-$(KH)_9$/pDNA complex (mito-RLuc), which was previously to successfully facilitate transfection into plant mitochondria.[17] Cytcox/KAibA-Mic demonstrated functions of mitochondrial targeting and membrane penetration, and thus, this micelle is a prospective gene carrier for increased transfection efficiency to plant mitochondria.

Transfection Efficiency of Cytcox/KAibA-Mic at Various Cytcox Modification Rates. Membrane permeability improves transfection efficiency but induces nonspecific interactions in the cell.[18] A gene carrier with high membrane permeability is effective for transfection to the nucleus but not selective for transfection to mitochondria. Therefore, control of the functions of mitochondrial targeting and membrane penetration is significant for efficient transfection into mitochondria. Cytcox/KAibA-Mic with quantified peptide modification rates was prepared and used to deliver pDNA to plant mitochondria. Then, we tried to prepare Cytcox/KAibA-Mic with controlled modification rates by changing the quantity of the cysteine-containing peptide reactant. In this experiment, the amount of Cys-KAibA added was constant under all modification conditions, and only that of Cytcox-Cys changed. Each peptide modification rate was quantified using HPLC as described above (Figure S6A–E). Although the Cytcox modification rates increased according to the amount of Cytcox-Cys added, the KAibA modification rates (9.1–10.4%) did not change significantly depending on the Cytcox modification rates (Table S4). This tendency indicated that the peptide modification rate was less affected by the modification of another peptide. For evaluating the transfection efficiency to the nucleus and mitochondria, *pDONR-Cox2-RLuc* and *pDONR-35S-RLuc* were used to prepare the peptide-modified micelles and complexes. The hydrodynamic diameters under each modification condition were measured by DLS (Figure 7A and Table S4). The sizes of Cytcox/KAibA-Mic prepared from either pDNA did not change significantly with the Cytcox modification rate. The plant cell wall has a network structure and physically protects the plant cell. The carrier size strongly affects cell wall permeability, and smaller carriers are more permeable.[32] In particular, since carriers with a diameter of 50 nm or less can easily penetrate the cell wall, the permeability significantly changes at approximately 50 nm.[33,34] The average sizes of Cytcox/KAibA-Mic at various Cytcox modification rates were found to be almost constant in this experiment, at approximately 80 nm for *pDONR-Cox2-RLuc* and approximately 105 nm for *pDONR-35S-RLuc*. The zeta-potentials of Cytcox/KAibA-Mic also did not change significantly with the Cytcox modification rate (Table S5). Therefore, it seemed that the size and surface charge had little effect on the transfection efficiency at various Cytcox modification rates. The transfection efficiency to mitochondria improved in response to the Cytcox modification rate (Figure 7B). On the other hand, the transfection efficiency to the nucleus changed little at various Cytcox modification rates. Cellular uptake depends on the

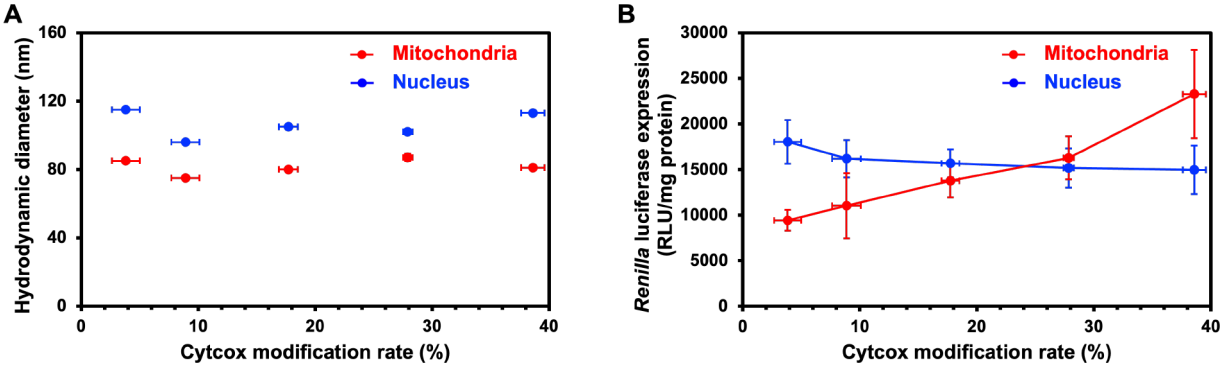

Figure 7. Quantitative evaluation of the transfection efficiency of Cytcox/KAibA-Mic at different Cytcox modification rates. (A) Hydrodynamic diameters of Cytcox/KAibA-Mic at each Cytcox modification rate ($n = 3$). The dots represent the mean under each condition. The vertical and horizontal error bars represent the standard error values of the hydrodynamic diameter and the Cytcox modification rate, respectively. (B) Transfection efficiency to the nucleus or mitochondria of Cytcox/KAibA-Mic versus the Cytcox modification rate ($n = 3$) based on the luciferase expression level ($n = 6$).

https://doi.org/10.1021/acs.biomac.3c00391
Biomacromolecules 2023, 24, 3657–3665

modification of KAibA.[29,35] In this report, we evaluated the transfection efficiency to the nucleus as an indicator of cellular uptake. Also, it has been reported that the transfection efficiency to mitochondria improved with an increase in the Cytcox presentation amount in the case of less than 15 nmol of Cytcox presentation amount in 820 μL peptide/DNA complex solution.[15] Considering the amount of added Cytcox-Cys and HPLC chromatograms at various Cytcox modification rates (Figure S6), the Cytcox presentation amount was less than 10 nmol in 820 μL Cytcox/KAibA-Mic solution. The results shown in Figure 7B implied that translocation to mitochondria depended on the Cytcox modification rate. Thus, the mode of gene introduction can be controlled by precisely preparing a gene carrier.

CONCLUSIONS

Low mitochondrial transfection efficiency has restricted mitochondrial transformation in plants. Efficient transfection into mitochondria requires the control of the functions of mitochondrial targeting and membrane penetration. In this research, we developed Cytcox/KAibA-Mic with controlled modification rates of mitochondrial targeting and cell membrane-penetrating peptides for transfection into plant mitochondria. With Cytcox/KAibA-Mic, the functions of mitochondrial targeting and membrane penetration could be controlled independently and quantitatively. Moreover, since Cytcox/KAibA-Mic was stable and maintained its size even when the modification rates changed, it could be used to compare the relationship more directly between the peptide modification rate and transfection efficiency. In this report, we evaluated the *Renilla* luciferase expression level as an indicator of transfection efficiency. When Cytcox/KAibA-Mic was introduced at different Cytcox modification rates, the transfection efficiency to the nucleus did not change, but the mitochondrial transfection efficiency increased with the modification rate (Figure 7B). The gene introduction efficiency and destination depend considerably on the carrier conditions. The accurate preparation of the gene carrier is important for efficiently introducing genes into the designated location. In Cytcox/KAibA-Mic, the transfection efficiency to mitochondria increased according to the increase of Cytcox modification rate (Figure 7B). However, Cytcox/KAibA-Mic at the Cytcox modification ratio of over 40% was unstable and could not be introduced to the plants. With respect to KAibA, increasing the KAibA modification rate would decrease mitochondrial selectivity. Considering the stability of Cytcox/KAibA-Mic and mitochondrial selectivity, the Cytcox modification rate of 39% and the KAibA modification rate of 9% are considered the most suitable (Figure 7B and Table S4). The search for better mitochondrial targeting peptides than Cytcox for transfection to plant mitochondria with improved efficiency is also a future challenge to be addressed. For this search, the efficiency of various mitochondrial targeting peptides needs to be quantitatively compared. As mentioned above, there are many challenges in mitochondrial transfection in plants. To optimize each condition, the quantification of modification rates and transfection efficiency is essential. The Cytcox/KAibA-Mic developed in this report can be used to quantify these parameters and has the potential to significantly contribute to improving transfection into plant mitochondria.

ASSOCIATED CONTENT

Supporting Information

The Supporting Information is available free of charge at https://pubs.acs.org/doi/10.1021/acs.biomac.3c00391.

Characterization of synthesized MAL-TEG-$(KH)_{14}$; design of plasmid DNA constructs used in this report; zeta-potential values of PD-Mic at different N/P ratios; RP-HPLC chromatograms of the reaction solution in preparation of Cytcox-Mic and KAibA-Mic; representative CLSM images of *A. thaliana* root cells infiltrated with pDNA, Cytcox-$(KH)_9$/pDNA complex, Cytcox-Mic, KAibA-Mic, and Cytcox/KAibA-Mic containing *pDONR-35S-GFP*; HPLC chromatograms used to quantify peptide modification rates at different Cytcox modification rates; z-average diameter, polydispersity index (PDI) values, and zeta-potential of PD-Mic at different N/P ratios; z-average diameter and PDI value of all peptide/DNA micelle complexes used in this report; zeta-potential values of Cytcox-Mic, KAibA-Mic, and Cytcox/KAibA-Mic; the hydrodynamic diameter of Cytcox/KAibA-Mic at different Cytcox modification rates; and zeta-potential of Cytcox/KAibA-Mic at different Cytcox modification rates (PDF)

AUTHOR INFORMATION

Corresponding Author

Keiji Numata − *Department of Material Chemistry, Graduate School of Engineering, Kyoto University, Kyoto 615-8510, Japan; Biomacromolecules Research Team, RIKEN Center for Sustainable Resource Science, Saitama 3510198, Japan;* orcid.org/0000-0003-2199-7420; Email: numata.keiji.3n@kyoto-u.ac.jp

Authors

Naoya Abe − *Department of Material Chemistry, Graduate School of Engineering, Kyoto University, Kyoto 615-8510, Japan*

Seiya Fujita − *Department of Material Chemistry, Graduate School of Engineering, Kyoto University, Kyoto 615-8510, Japan*

Takaaki Miyamoto − *Biomacromolecules Research Team, RIKEN Center for Sustainable Resource Science, Saitama 3510198, Japan;* orcid.org/0000-0002-8192-9342

Kousuke Tsuchiya − *Department of Material Chemistry, Graduate School of Engineering, Kyoto University, Kyoto 615-8510, Japan*

Complete contact information is available at: https://pubs.acs.org/10.1021/acs.biomac.3c00391

Author Contributions

S.F., T.M., K.T., and K.N. conceived and designed the research. N.A. and K.N. wrote the manuscript. N.A. performed all the experiments and analyzed the data.

Notes

The authors declare no competing financial interest.

ACKNOWLEDGMENTS

This work was supported by JST-ERATO Grant Number JPMJER1602, JST-COI-NEXT, and MEXT Data Creation and Utilization-type MaTerial R&D project.

REFERENCES

(1) Godfray, H. C.; Beddington, J. R.; Crute, I. R.; Haddad, L.; Lawrence, D.; Muir, J. F.; Pretty, J.; Robinson, S.; Thomas, S. M.; Toulmin, C. Food security: the challenge of feeding 9 billion people. *Science* **2010**, *327*, 812−818.
(2) Tilman, D.; Balzer, C.; Hill, J.; Befort, B. L. Global food demand and the sustainable intensification of agriculture. *Proc. Natl. Acad. Sci. U. S. A.* **2011**, *108*, 20260−20264.
(3) Foley, J. A.; Ramankutty, N.; Brauman, K. A.; Cassidy, E. S.; Gerber, J. S.; Johnston, M.; Mueller, N. D.; O'Connell, C.; Ray, D. K.; West, P. C.; et al. Solutions for a cultivated planet. *Nature* **2011**, *478*, 337−342.
(4) Altpeter, F.; Baisakh, N.; Beachy, R.; Bock, R.; Capell, T.; Christou, P.; Daniell, H.; Datta, K.; Datta, S.; Dix, P. J.; et al. Particle bombardment and the genetic enhancement of crops: myths and realities. *Mol. Breed.* **2005**, *15*, 305−327.
(5) Nonaka, S.; Ezura, H. Plant-Agrobacterium interaction mediated by ethylene and super-Agrobacterium conferring efficient gene transfer. *Front. Plant Sci.* **2014**, *5*, 681.
(6) Weising, K.; Schell, J.; Kahl, G. Foreign genes in plants: transfer, structure, expression, and applications. *Annu. Rev. Genet.* **1988**, *22*, 421−477.
(7) Mackenzie, S. A.; Pring, D. R.; Bassett, M. J.; Chase, C. D. Mitochondrial DNA rearrangement associated with fertility restoration and cytoplasmic reversion to fertility in cytoplasmic male sterile Phaseolus vulgaris L. *Proc. Natl. Acad. Sci. U. S. A.* **1988**, *85*, 2714−2717.
(8) Larosa, V.; Remacle, C. Transformation of the mitochondrial genome. *Int. J. Dev. Biol.* **2013**, *57*, 659−665.
(9) Yoshinaga, N.; Numata, K. Rational Designs at the Forefront of Mitochondria-Targeted Gene Delivery: Recent Progress and Future Perspectives. *ACS Biomater. Sci. Eng.* **2022**, *8*, 348−359.
(10) Numata, K. *Biopolymer science for proteins and peptides*; Elsevier: Amsterdam, 2021.
(11) Hurt, E. C.; Pesoldhurt, B.; Schatz, G. The Cleavable Prepiece of an Imported Mitochondrial Protein Is Sufficient to Direct Cytosolic Dihydrofolate-Reductase into the Mitochondrial Matrix. *FEBS Lett.* **1984**, *178*, 306−310.
(12) Schatz, G.; Dobberstein, B. Common principles of protein translocation across membranes. *Science* **1996**, *271*, 1519−1526.
(13) Keegstra, K.; Cline, K. Protein import and routing systems of chloroplasts. *Plant Cell* **1999**, *11*, 557−570.
(14) Hurt, E. C.; Pesold-Hurt, B.; Suda, K.; Oppliger, W.; Schatz, G. The first twelve amino acids (less than half of the pre-sequence) of an imported mitochondrial protein can direct mouse cytosolic dihydrofolate reductase into the yeast mitochondrial matrix. *EMBO J.* **1985**, *4*, 2061−2068.
(15) Chuah, J. A.; Yoshizumi, T.; Kodama, Y.; Numata, K. Gene introduction into the mitochondria of Arabidopsis thaliana via peptide-based carriers. *Sci. Rep.* **2015**, *5*, 7751.
(16) Chuah, J. A.; Matsugami, A.; Hayashi, F.; Numata, K. Self-Assembled Peptide-Based System for Mitochondrial-Targeted Gene Delivery: Functional and Structural Insights. *Biomacromolecules* **2016**, *17*, 3547−3557.
(17) Yoshizumi, T.; Oikawa, K.; Chuah, J. A.; Kodama, Y.; Numata, K. Selective Gene Delivery for Integrating Exogenous DNA into Plastid and Mitochondrial Genomes Using Peptide-DNA Complexes. *Biomacromolecules* **2018**, *19*, 1582−1591.
(18) Law, S. S. Y.; Liou, G.; Nagai, Y.; Gimenez-Dejoz, J.; Tateishi, A.; Tsuchiya, K.; Kodama, Y.; Fujigaya, T.; Numata, K. Polymer-coated carbon nanotube hybrids with functional peptides for gene delivery into plant mitochondria. *Nat. Commun.* **2022**, *13*, 2417.
(19) Morris, M. C.; Chaloin, L.; Heitz, F.; Divita, G. Translocating peptides and proteins and their use for gene delivery. *Curr. Opin. Biotechnol.* **2000**, *11*, 461−466.
(20) Gariepy, J.; Kawamura, K. Vectorial delivery of macromolecules into cells using peptide-based vehicles. *Trends Biotechnol.* **2001**, *19*, 21−28.
(21) Katayose, S.; Kataoka, K. Water-soluble polyion complex associates of DNA and poly(ethylene glycol)-poly(L-lysine) block copolymer. *Bioconjugate Chem.* **1997**, *8*, 702−707.
(22) Chen, C. P.; Chou, J. C.; Liu, B. R.; Chang, M.; Lee, H. J. Transfection and expression of plasmid DNA in plant cells by an arginine-rich intracellular delivery peptide without protoplast preparation. *FEBS Lett.* **2007**, *581*, 1891−1897.
(23) Hashemi, M.; Parhiz, B. H.; Hatefi, A.; Ramezani, M. Modified polyethyleneimine with histidine-lysine short peptides as gene carrier. *Cancer Gene Ther.* **2011**, *18*, 12−19.
(24) Lakshmanan, M.; Kodama, Y.; Yoshizumi, T.; Sudesh, K.; Numata, K. Rapid and efficient gene delivery into plant cells using designed peptide carriers. *Biomacromolecules* **2013**, *14*, 10−16.
(25) Lakshmanan, M.; Yoshizumi, T.; Sudesh, K.; Kodama, Y.; Numata, K. Double-stranded DNA introduction into intact plants using peptide-DNA complexes. *Plant Biotechnol.* **2015**, *32*, 39−45.
(26) Thagun, C.; Chuah, J. A.; Numata, K. Targeted Gene Delivery into Various Plastids Mediated by Clustered Cell-Penetrating and Chloroplast-Targeting Peptides. *Adv. Sci.* **2019**, *6*, No. 1902064.
(27) Miyamoto, T.; Tsuchiya, K.; Numata, K. Dual Peptide-Based Gene Delivery System for the Efficient Transfection of Plant Callus Cells. *Biomacromolecules* **2020**, *21*, 2735−2744.
(28) Thagun, C.; Motoda, Y.; Kigawa, T.; Kodama, Y.; Numata, K. Simultaneous introduction of multiple biomacromolecules into plant cells using a cell-penetrating peptide nanocarrier. *Nanoscale* **2020**, *12*, 18844−18856.
(29) Miyamoto, T.; Tsuchiya, K.; Numata, K. Endosome-escaping micelle complexes dually equipped with cell-penetrating and endosome-disrupting peptides for efficient DNA delivery into intact plants. *Nanoscale* **2021**, *13*, 5679−5692.
(30) Odahara, M.; Horii, Y.; Itami, J.; Watanabe, K.; Numata, K. Functional peptide-mediated plastid transformation in tobacco, rice, and kenaf. *Front. Plant Sci.* **2022**, *13*, No. 989310.
(31) Fields, G. B.; Noble, R. L. Solid phase peptide synthesis utilizing 9-fluorenylmethoxycarbonyl amino acids. *Int. J. Pept. Protein Res.* **1990**, *35*, 161−214.
(32) Zhang, H.; Goh, N. S.; Wang, J. W.; Pinals, R. L.; Gonzalez-Grandio, E.; Demirer, G. S.; Butrus, S.; Fakra, S. C.; Del Rio Flores, A.; Zhai, R.; et al. Nanoparticle cellular internalization is not required for RNA delivery to mature plant leaves. *Nat. Nanotechnol.* **2022**, *17*, 197−205.
(33) Eichert, T.; Kurtz, A.; Steiner, U.; Goldbach, H. E. Size exclusion limits and lateral heterogeneity of the stomatal foliar uptake pathway for aqueous solutes and water-suspended nanoparticles. *Physiol. Plant.* **2008**, *134*, 151−160.
(34) Zhi, H.; Zhou, S.; Pan, W.; Shang, Y.; Zeng, Z.; Zhang, H. The Promising Nanovectors for Gene Delivery in Plant Genome Engineering. *Int. J. Mol. Sci.* **2022**, *23*, 8501.
(35) Terada, K.; Gimenez-Dejoz, J.; Miyagi, Y.; Oikawa, K.; Tsuchiya, K.; Numata, K. Artificial Cell-Penetrating Peptide Containing Periodic alpha-Aminoisobutyric Acid with Long-Term Internalization Efficiency in Human and Plant Cells. *ACS Biomater. Sci. Eng.* **2020**, *6*, 3287−3298.

https://doi.org/10.1021/acs.biomac.3c00391
Biomacromolecules 2023, 24, 3657−3665